Energy Systems Planning and Optimization

Journal home page: https://espo.kut.ac.ir

Research paper

The Impact of Convergent-Divergent Nozzle Geometry on Thrust for Fuel Consumption Optimization

Amin Nabati [1*], Morteza Saadat Targhi [1], Narges Malek Nia [2]

[1] *Mechanical Engineering Department, Esfarayen University of Technology, Esfarayen, Iran*

[2] *Master's student of Mechanical Engineering, Khajeh Nasir al-Din Toosi University of Technology, Tehran, Iran.*

Article Info

Received
18 March 2026

Revised
7 May 2026

Accepted
8 Jun 2026

Published online
21 Jun 2026

Keywords

Converging-diverging nozzle;
Propulsion force;
Mach number;
Throat

Abstract

Convergent-divergent nozzles are critical components in rocket and jet propulsion systems, designed to decelerate and de-pressure exhaust gases, thereby accelerating them to supersonic speeds and generating thrust. This study investigates the impact of convergent–divergent nozzle geometry on thrust performance through two-dimensional, compressible airflow simulations using Ansys Fluent. Two distinct nozzle geometries—one with a curved wall and another with an inclined wall—are analyzed. Flow characteristics are simulated under a constant inlet air temperature of 1200 K across five inlet pressure conditions: 5, 10, 15, 20, and 40 bar. The nozzle walls are assumed to be insulated, and the inlet, throat, and outlet cross-sectional areas are maintained consistently across both geometries. Simulation results indicate that the Mach number at the nozzle exit is consistently higher for the inclined-wall geometry compared to the curved-wall geometry, whereas the opposite trend is observed at the throat. With an increase in inlet pressure from 5 to 15 bar, the exit Mach number for both geometries shows a notable increase. However, beyond 15 bar, the exit Mach number plateaus, suggesting a saturation point. Thrust generation in both designs demonstrated a significant increase with rising inlet pressure. While the inclined-wall nozzle produced greater thrust at inlet pressures below 20 bar, the curved-wall nozzle exhibited superior thrust performance at the highest tested pressure of 40 bar.

* Corresponding author's Email address: a.nabati@esfarayen.ac.ir

 https://doi.org/10.22034/espo.2026.2086952.1004

1. Introduction

Convergent–divergent (C-D) nozzles are integral to propulsion systems, as they efficiently convert the thermal and pressure energy generated within the combustion chamber into kinetic energy of the exhaust flow, thereby producing thrust. The performance of these nozzles is influenced by a several factors, including fluid properties, inlet temperature and pressure, ambient pressure, nozzle geometry, and the area ratios of the inlet, throat, and outlet sections. Given their critical role, numerous studies have explored and characterized the performance of C-D nozzles. The following section reviews relevant prior research in this domain.

Ghorbanzadeh and Lakzian [1] demonstrated that using a C-D nozzle in an ejector, compared with a purely convergent nozzle, yields better ejector performance in terms of more efficient energy utilization and increased suction of the secondary flow. Babaeyan and Hojaji [2] experimentally investigated the effects of dual protrusions in a C-D nozzle operating in a supersonic regime. Their results showed that opposite-facing dual protrusions reduce the thrust loss by about 5 % and significantly affected the thrust-vector angle. Sharifi and Mokhtari [3] experimentally evaluated the impact of several unconventional obstacles cube-shaped, spherical, cylindrical and conical on the thrust vector of a C-D nozzle. The cubic obstacle produced the largest thrust deviation, whereas all obstacles caused a slight reduction in axial thrust. Fakhari et al. [4] numerically and experimentally examined how the geometry of the divergent section affects the internal flow and heat transfer in a C-D nozzle. Two nozzles were studied: one with a conical divergent part and another with a bell-shaped divergent part. Results indicated that the thrust produced by the conical nozzle is higher than that of the bell-shaped nozzle. Rahaei et al. [5] investigated transient flow, heat transfer, and thrust in C-D nozzles with various geometries. With a fixed nozzle length, increasing the divergence angle raised the exit Mach number while decreasing exit pressure and temperature. Compared with conical nozzles, Bell-shaped nozzle exhibited higher exit Mach numbers and lower exit temperature and pressure. Furthermore, reducing the exit-section angle in a bell-shaped nozzle increased the Mach number and thrust while lowering the exit temperature and pressure. The surface temperature at the exit was higher for the bell-shaped nozzle than for the conical nozzle.

Khan et al. [6] performed numerical simulations of airflow inside a C-D nozzle equipped with a downstream channel and examined the effects of the inlet-pressure ratio influences temperature, pressure, velocity, and density distributions along the nozzle. Mahmoodi and Rafie [7] studied the compressible flow behavior in various C-D nozzle geometries. In all cases, the ratio of exit-area to throat-area and the total combustion-chamber pressure were kept constant, while the nozzle shape varied. Four configurations were examined: an optimal-path nozzle, a 15° conical nozzle, a 30° conical nozzle, and a short-length nozzle. Under design conditions, the optimal-path nozzle generated the highest thrust (≈ 7 889 N). However, in off-design conditions the 30° conical nozzle produced the highest thrust (≈ 9 700 N) among the studied designs. Afkhami et al. [8] carried out numerical simulations of airflow in an optimally-shaped parabolic (TRUST) nozzle. They first evaluated flow separation using conventional turbulence models and then refined the turbulence parameters. The modified turbulence model proved highly capable of accurately predicting flow physics and the location of flow separation.

Esmaeili et al. [9] examined the effect of varying the expansion ratio of a C-D nozzle on specific impulse, exit velocity, and exit temperature for different propellants using thermodynamic relations. Their results showed that increasing the expansion ratio leads to nonlinear increases in specific impulse, exit velocity, exit Mach number, and thrust coefficient, while the exit temperature decreases. Hajaji et al. [10] observed and investigated the flow in an inclined convergent–divergent (C-D) nozzle with the injection of multiple secondary flows. Three inclined C-D nozzle geometries with angles of 25°, 45°, and 65° relative to the exit cross-section were evaluated. The results showed that, for a constant initial pressure, increasing the secondary injection pressure increased the deflection angle, but the rate of this increase was much lower for the 65° inclined C-D nozzle than for the other two angles.

Arzini and Nimafar [11] investigated two-dimensional single-flow in a C-D nozzle with a constant convergent angle and varying divergent geometries. Three Radius curvature (10, 35, and 75 mm) and three different angles (4.7°, 9°, and 15°) were considered. The results showed that the radius of curvature has little effect on the Mach number and pressure, but increasing the divergence angle increases the exit Mach number. Farshi Fasih and Kamrava [12] numerically investigated the effect of changing the nozzle throat diameter on the fluid flow inside a C-D nozzle. The simulation was performed bidimensional using Fluent software for a single-phase turbulent flow and steady-state conditions. The results indicated that increasing the nozzle throat diameter changes the exit Mach number, temperature, and pressure of the nozzle.

Pourtaghi Marzrood et al. [13] investigated the flow of butane propellant in a C-D nozzle with optimized dimensions to determine the appropriate area expansion ratio. The results showed that increasing the area expansion ratio decreases the average axial velocity at the exit cross-section. Also, increasing the thrust is achieved by decreasing the area expansion ratio of the nozzle and reducing the backflow. Hamidi and Kermani [14] numerically investigated the effect of the geometry of the C-D nozzle and static conditions on the moisture formation and nucleation rate. The results show that increasing the area expansion ratio of the nozzle causes earlier condensation, and also increases the nucleation rate and moisture output from the nozzle.

Bagherzadeh et al. [15] designed an optimized profile for the divergent section of a supersonic nozzle with the aim of achieving maximum thrust while maintaining the length and the exit-to-throat area ratio of the nozzle. The results showed that the optimized designed nozzle performs better than the conventional nozzle up to a pressure ratio of 30, but at pressure ratios greater than 30, the performance of both nozzles is similar. Mohammad Hasan Zadeh et al. [16] simulated and analyzed the effect of secondary fluid injection in the nozzle on the nozzle thrust vector. They showed that the inlet pressure, injection flow rate, injection position, and injection angle are the most important parameters affecting the change in the thrust vector angle in the nozzle. Bellary et al. [17] used computational fluid dynamics to study the flow inside a stepped C-D nozzle at various divergence angles between 5° and 13.5° with a constant throat diameter. The results showed that the divergence angle has a significant effect on the back pressure and Mach number. Also, 13.5° was identified as the optimal divergence angle for maximum velocity. Guangtao et al. [18] showed that using two identical C-D nozzles side by side creates a beneficial interaction effect between the dual jets, resulting in increased thrust and lift. The overall performance of the combined nozzle outperformed the two nozzles operating independently. Teixeira et al. [19] numerically investigated the performance of novel contoured nozzles and showed that, compared with conventional conical C-D nozzles, they increased the exit Mach number by 19% and reduce the entropy loss by 7.3%.

This study investigates the influence of C-D nozzle geometry on aerodynamic performance using computational fluid dynamics (CFD) simulations. Two distinct nozzle geometries, featuring curved and inclined walls, are analyzed. To ensure a fair comparison, the inlet, throat, and outlet cross-sectional areas are maintained identically for both designs. The flow behavior within these nozzles is simulated across a range of inlet pressures, specifically 5, 10, 15, 20, and 40 bar.

2. Modeling and Simulation

In this study, the C-D nozzle geometries are modeled using ANSYS SpaceClaim. Two distinct wall configurations curved and inclined are designed to evaluate nozzle performance (Figure 1). For both designs, the inlet and outlet diameters are maintained at 25 mm, while the throat diameter is set at 25.6 mm. The total length of the nozzles is established at 75 mm, with the throat positioned at the midsection. For the curved-wall configuration, the wall profile is defined with a radius of curvature of 120 mm.

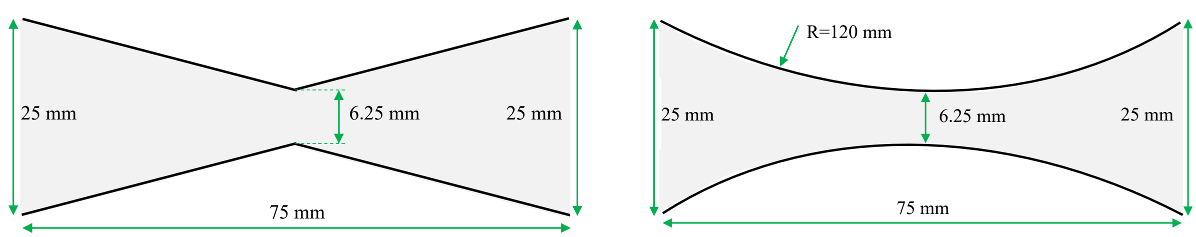

(a) (b)

Fig. 1. Geometrical model of convergent-divergent nozzle (a) nozzle with slanted wall (b) nozzle with curved wall

To facilitate flow simulation and numerical analysis, a computational mesh is generated within the defined geometry. The mesh employed for both nozzle configurations is structured, rectangular, and comprises 18,774 elements. Recognizing the critical influence of flow phenomena near the walls and at the throat, a boundary layer mesh is implemented in these regions to ensure adequate resolution. Figure 2 illustrates the computational mesh, including a detailed view of the mesh near the throat of the inclined-wall convergent–divergent nozzle.

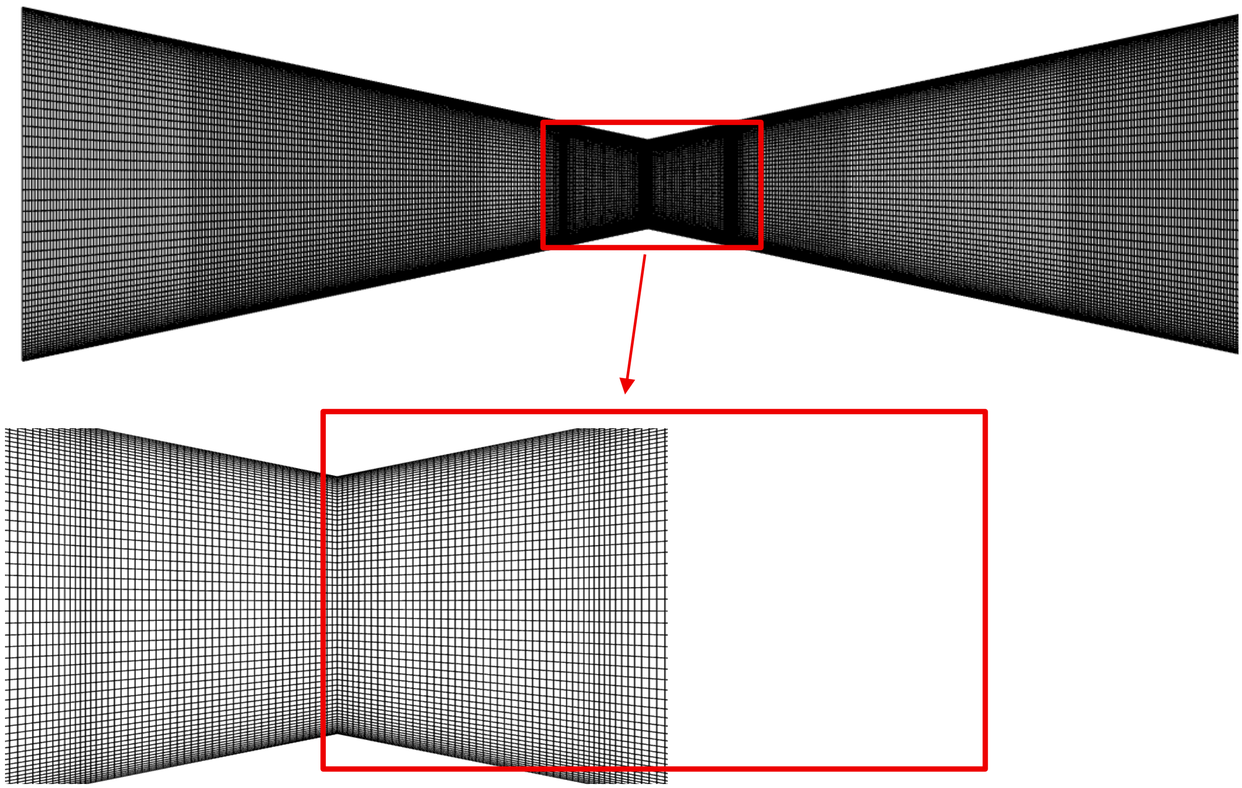

Fig. 2. The mesh created in the computational space for the convergent-divergent nozzle with a slanted wall and a closer view at the throat

To assess the quality of the mesh, the independence of the results from the generated mesh is evaluated. Table 1 presents the results of the mesh quality assessment. The results indicate that mesh number 2, with 18,774 elements, is suitable for both computational spaces.

Table 1. Mach number at the exit of both nozzles for three different grids

Grid	Element Number	Output Mach for 5-bar inlet pressure		Output Mach for 40-bar inlet pressure	
		Nozzle with slanted wall	Nozzle with curved wall	Nozzle with slanted wall	Nozzle with curved wall
Mesh 1	12,224	0.82	0.58	2.87	2.84
Mesh 2	18,774	0.83	0.57	2.88	2.85
Mesh 3	26,726	0.83	0.57	2.88	2.85

Furthermore, to ensure the quality of the mesh, three metrics namely, aspect ratio, skewness, and orthogonality were evaluated. The final values of the aspect ratio, skewness, and orthogonality for the nozzles were 1.4, 0.08, and 0.92, respectively indicating that generated mesh enjoyed a satisfactory quality. To analyze the flow inside the nozzle, the governing equations for fluid flow must be solved in the discretized computational space. These governing equations for fluid flow include the continuity, momentum, and energy equations, which for air inside the nozzle are as follows [20].

$$\frac{\partial \rho}{\partial t} + \frac{\partial (\rho u_i)}{\partial x_i} = 0 \tag{1}$$

$$\frac{\partial (\rho u_i)}{\partial t} + \frac{\partial (\rho u_i u_j)}{\partial x_j} = \frac{\partial p}{\partial x_i} - \frac{\partial (\rho \overline{u_i u_j})}{\partial x_i} + \frac{\partial}{\partial x_j}\left(\mu \frac{\partial u_i}{\partial x_j}\right) \tag{2}$$

$$\frac{\partial (\rho c_p T)}{\partial t} + \frac{\partial (\rho c_p u_j T)}{\partial x_j} = -\tau_{ij}\frac{\partial u_i}{\partial x_j} + \frac{\partial}{\partial x_j}\left(\lambda \frac{\partial T}{\partial x_j}\right) \tag{3}$$

In these equations, ρ is the fluid density, u represents the velocity components of the fluid, p is the pressure, c_p is the specific heat, T is the fluid temperature, μ is the fluid viscosity, λ is the thermal conductivity, and $\tau_{ij} = -\rho\overline{u_i u_j}$ is the Reynolds stress tensor, which is obtained from the following relation.

$$\tau_{ij} = -\frac{2}{3}\mu \frac{\partial u_i}{\partial x_i}\delta_{ij} + \mu\left(\frac{\partial u_j}{\partial x_i} + \frac{\partial u_i}{\partial x_j}\right) \tag{4}$$

In this research, the k-ω turbulence model is used. This model consists of two equations for calculating the turbulence kinetic energy (k) and the rate of dissipation of turbulence kinetic energy (ω). The equations related to these parameters are as follows [20].

$$\frac{\partial (\rho k)}{\partial t} + \frac{\partial (\rho k u_j)}{\partial x_j} = \frac{\partial}{\partial x}\left(\mu + \frac{\mu_t}{\sigma_k}\right)\frac{\partial k}{\partial x_i} - \frac{2}{3}\rho k \frac{\partial (\rho u_i)}{\partial x_j}\delta_{ij} + \tau_{ij}S_{ij} - \beta^* \rho k \omega \tag{5}$$

$$\frac{\partial (\rho \omega)}{\partial t} + \frac{\partial (\rho \omega u_j)}{\partial x_j} = \frac{\partial}{\partial x}\left(\mu + \frac{\mu_t}{\sigma_{\omega,1}}\right)\frac{\partial \omega}{\partial x_i} - \frac{2}{3}\rho \omega \frac{\partial (\rho u_i)}{\partial x_j}\delta_{ij}\gamma_2 + 2\rho \tau_{ij}S_{ij}\gamma_2 - \beta_2 \rho \omega^2 + 2\frac{\rho}{\sigma_{\omega,2}}\frac{\partial k}{\partial x_k}\frac{\partial \omega}{\partial x_k} \tag{6}$$

The constant values for σ_k, σ_ω, γ_2, β_2, and β^* are 2, 1.17, 0.44, 0.083, and 0.009, respectively.

This study investigated the flow characteristics within C-D nozzles by simulating the internal flow field to determine the outlet Mach number and thrust. Two nozzle geometries, one with inclined walls and another with curved walls, were considered. A density-based, steady-state solver was utilized, suitable for the compressible flow regime within the nozzle. The simulation assumed insulated walls and employed pressure boundary conditions at both the inlet and outlet. The working fluid was modeled as air, treated as a compressible and steady medium with a constant inlet temperature of 1200 K. Five distinct inlet pressure conditions are evaluated: 5, 10, 15, 20, and 40 bar.

Given the expected high velocities, the flow was assumed to be turbulent, necessitating the use of the k-ω shear stress transport (SST) turbulence model. This model is known for its robustness and accuracy in predicting complex flow phenomena, including adverse pressure gradients often encountered in nozzle flows. A coupled pressure-velocity coupling algorithm was utilized, and the governing equations for fluid flow are discretized using the second-order upwind discretization scheme.

Convergence was established when the residuals for all governing equations (continuity, momentum, energy, k, and ω) dropped below a stringent threshold of 10^{-5}. In addition to residual monitoring, key integral quantities such as the total thrust generated by the nozzle and the mass flow rate at the exit were continuously monitored.

Although a convergent–divergent nozzle is inherently a three-dimensional problem from both geometric and physical perspectives, it can be modeled accurately using a two-dimensional problem under the following conditions: (1) the nozzle is perfectly axisymmetric about its centerline, (2) the inlet flow conditions are uniform around the circumference, and (3) there is no side injection, thrust-vector deflection, or asymmetric flow disturbance. Under these assumptions, all flow properties, including pressure, temperature, velocity, and density, remain unchanged in the circumferential direction (θ). Consequently, the flow field depends only on the axial coordinate and the radial coordinate of the nozzle, allowing the three-dimensional problem to be reduced to a two-dimensional one with a high degree of accuracy.

Figure 3 displays the pressure distribution obtained from the ANSYS Fluent flow analysis for both investigated nozzle geometries across the evaluated inlet pressures. A notable observation is the uniform pressure distribution within the convergent section of both nozzles. In contrast, in the divergent section, a pressure decrease is observed near the walls, indicating wall influence on the flow field. This wall effect is more pronounced at lower inlet pressures and appears to be greater in the nozzle with curved walls compared to the inclined-wall configuration.

3. Results and discussion

In this research, the performance of two nozzles with inclined and curved walls is compared based on computational fluid dynamics simulations performed using ANSYS Fluent. Before presenting the results, the simulation results were validated against the findings of research by Bellary et al. [17]. Figure 4 compares the Mach number distribution along the nozzle axis obtained in this study with the corresponding results reported by Bellary et al. [17]. The close agreement between the present results and those from the reference [17] confirms the validity and accuracy of the numerical simulation methodology.

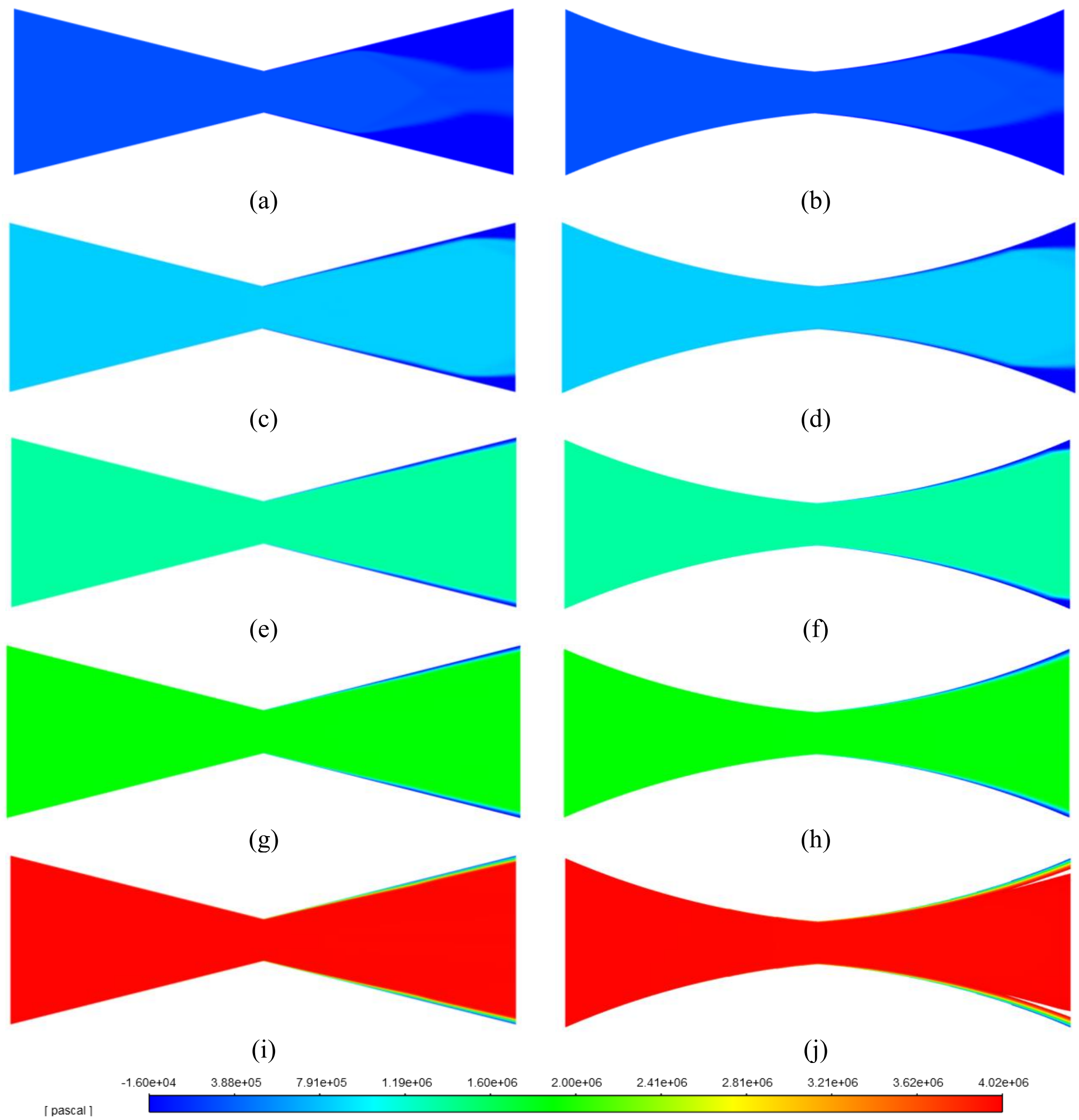

Fig. 3. Pressure distribution in the convergent-divergent nozzle: (a) with a slanted wall and an inlet air pressure of 5 bar, (b) with a curved wall and an inlet air pressure of 5 bar, (c) with a slanted wall and an inlet air pressure of 10 bar, (d) with a curved wall and an inlet air pressure of 10 bar, (e) with a slanted wall and an inlet air pressure of 15 bar, (f) with a curved wall and an inlet air pressure of 15 bar, (g) with a slanted wall and an inlet air pressure of 20 bar, (h) with a curved wall and an inlet air pressure of 20 bar, (i) with a slanted wall and an inlet air pressure of 40 bar, (j) with a curved wall and an inlet air pressure of 40 bar.

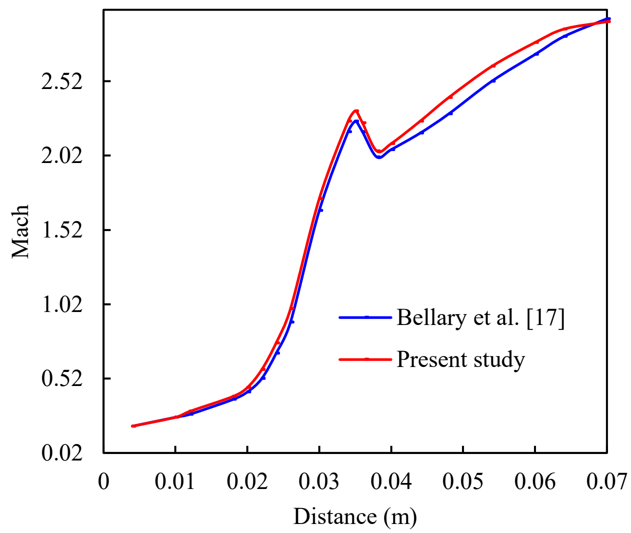

Fig. 4. Comparison of the results of the simulation conducted in this study with the results of Bellary et al. [17].

Figure 5 illustrates the Mach number distribution within the C-D nozzle across various inlet pressure conditions. It is observed that while the Mach number remains relatively constant throughout the convergent section and at the throat regardless of inlet pressure, it exhibits significant variation within the divergent section. Specifically, higher inlet pressures lead to increased Mach numbers in the divergent region, resulting in a more uniform flow profile at the exit. Furthermore, at lower inlet pressures, the flow separation or nucleation region in the divergent section is more pronounced.

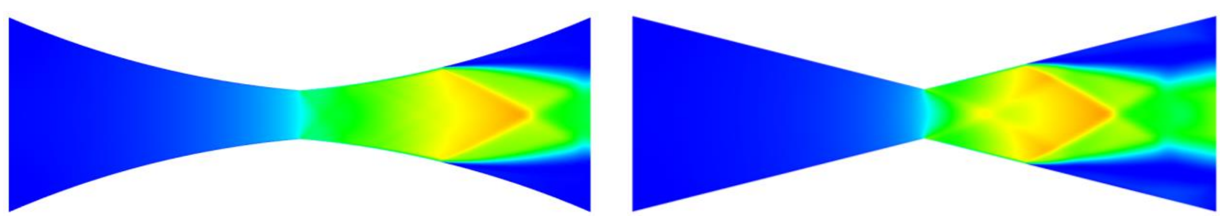

(a) (b)

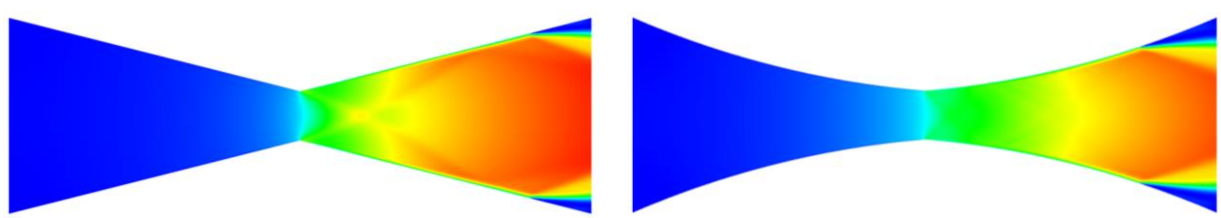

(c) (d)

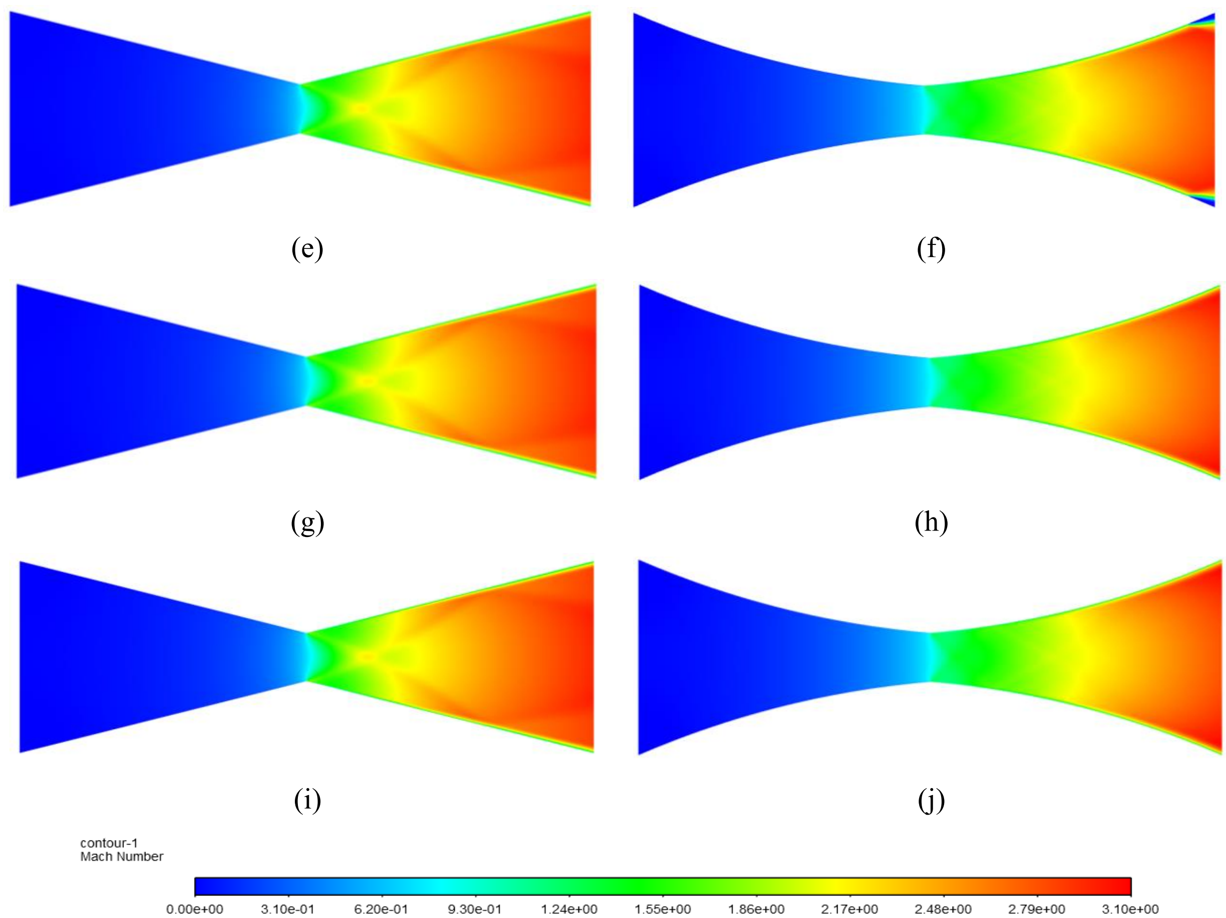

Fig. 5. Mach number distribution in the convergent-divergent nozzle: (a) with a slanted wall and an inlet air pressure of 5 bar, (b) with a curved wall and an inlet air pressure of 5 bar, (c) with a slanted wall and an inlet air pressure of 10 bar, (d) with a curved wall and an inlet air pressure of 10 bar, (e) with a slanted wall and an inlet air pressure of 15 bar, (f) with a curved wall and an inlet air pressure of 15 bar, (g) with a slanted wall and an inlet air pressure of 20 bar, (h) with a curved wall and an inlet air pressure of 20 bar, (i) with a slanted wall and an inlet air pressure of 40 bar, (j) with a curved wall and an inlet air pressure of 40 bar.

Figure 6 illustrates the nozzle exit Mach number as a function of inlet air pressure for both nozzle geometries. Consistently across all tested inlet pressures, the inclined-wall nozzle achieves a higher exit Mach number compared to the curved-wall nozzle. The exit Mach number increases with rising inlet air pressure up to 20 bar, beyond which it remains constant. Consequently, under the simulated conditions, the maximum achievable exit Mach number approaches approximately 2.85, indicating a saturation point where further increases in inlet pressure do not yield a higher exit Mach number.

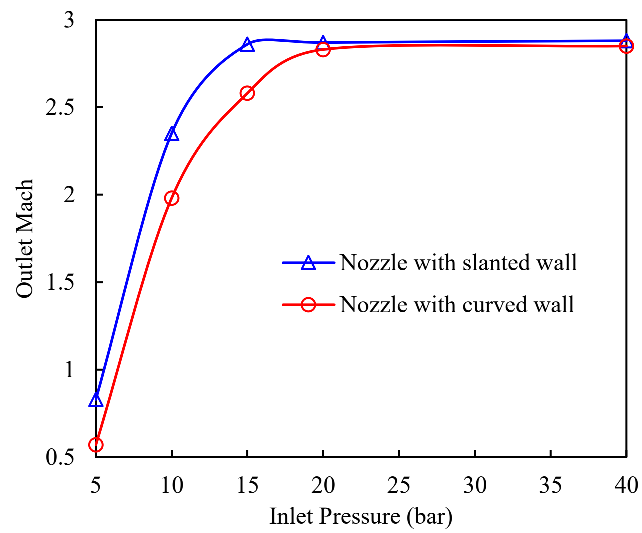

Fig. 6. Mach number at the outlet of the two nozzles under study varies with different inlet pressures.

Figure 7 shows the changes in Mach number at the throat as a function of inlet pressure for both nozzles. As observed, the Mach number at the throat is constant for each nozzle. However, contrary to the conditions of the Mach number at the nozzle outlet, this graph shows that the Mach number at the throat of the curved-wall nozzle is always higher than that of the inclined-wall nozzle.

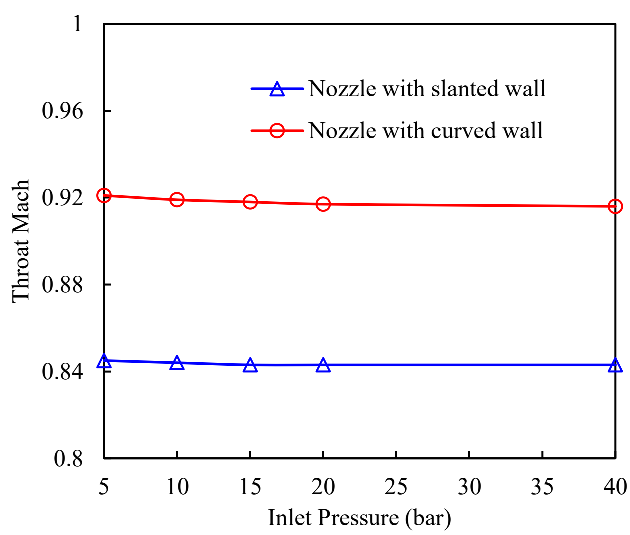

Fig. 7. Mach number at the throat of the two nozzles under study varies with different inlet pressures.

Figure 8 presents the variation in exit air temperature for both nozzle configurations at different inlet pressures. The results show that at inlet pressures of 5 to 15 bar, the outlet temperature of the inclined-wall nozzle is higher than that of the curved-wall nozzle. However, at higher inlet pressures of 20 to 40 bar, this trend reverses slightly, and the curved-wall nozzle exhibits a marginally higher exit air temperature than the inclined-wall nozzle.

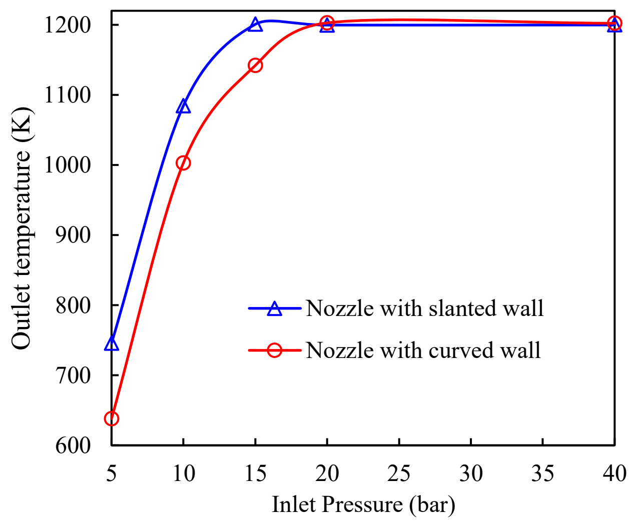

Fig. 8. Outlet temperature of the two nozzles under study varies with different inlet pressures.

One of the key parameters affecting the fuel consumption of aerospace propulsion systems is the thrust force generated at the exit of the convergent–divergent nozzle. The thrust force is calculated using the following equation:

$$F = \dot{m}V_e + (P_e - P_a)A_e \quad (7)$$

where m is the outlet mass flow rate, V_e is the exit velocity, P_e is the exit pressure, P_a is the ambient pressure, and A_e is the nozzle exit area.

The changes in thrust force generated in the nozzles as a function of inlet pressure are shown in Figure 9. As the inlet pressure rises, the thrust in both nozzles increases. At inlet pressures of 5 to 20 bar, the thrust generated in the inclined-wall nozzle is greater than that in the curved-wall nozzle, but at 40 bar, the thrust in the curved-wall nozzle becomes greater. Therefore, for lower fuel consumption, it is recommended to use a nozzle with an inclined wall for pressures below 20 bar, and a nozzle with a curved wall for pressures above 20 bar.

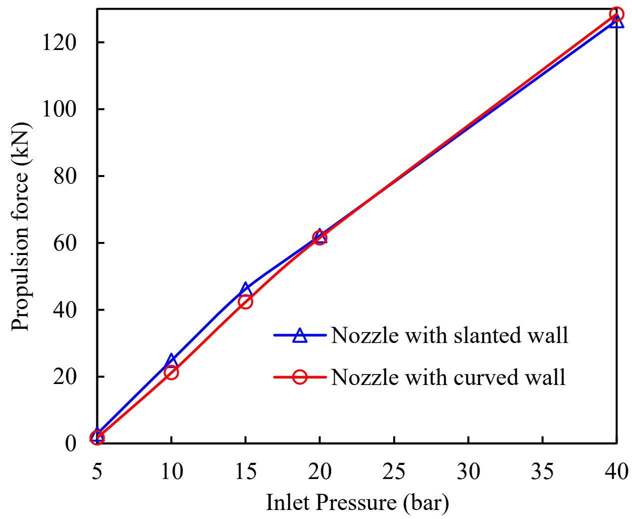

Fig. 9. Propulsion force of the two nozzles under study varies with different inlet pressures.

4. Conclusions

This research investigated the impact of convergent–divergent nozzle geometry—specifically inclined-wall versus curved-wall configurations—on the exit Mach number and thrust generated across a range of inlet pressures. Airflow simulations were conducted using ANSYS Fluent for five distinct inlet pressures: 5, 10, 15, 20, and 40 bar.

The simulation results indicated that while the Mach number at the nozzle throat remained constant with increasing inlet pressure, a notable trend emerged at the outlet. The exit Mach number increased up to an inlet pressure of 20 bar, after which it plateaued. Interestingly, the curved-wall nozzle exhibits a higher Mach number at the throat, whereas the inclined-wall nozzle achieved a higher Mach number at the exit. Furthermore, thrust generally increased significantly for both nozzle types with rising inlet pressure. While thrust values were comparable between the two geometries, the inclined-wall nozzle generated greater thrust at inlet pressures from 5 to 20 bar, whereas the curved-wall nozzle produced slightly higher thrust at the highest inlet pressure of 40 bar. Therefore, for pressures below 20 bar, employing a nozzle with an inclined wall led to lower fuel consumption, but at pressures above 20 bar, using a nozzle with a curved wall resulted in reduced fuel consumption.

Authors' contributions

Amin Nabati1: *Data curation, Writing- Original draft preparation, Investigation*

Morteza Saadat Targhi*:* Supervision, Methodology, Writing- Reviewing and Editing

Narges Malek Nia: Software

Funding

The authors did not receive support from any organization for the submitted work.

Declaration of competing interest

The authors declare that they have no known competing financial interests or personal relationships that could have appeared to influence the work reported in this paper.

Availability of data and materials

All data, models, or code generated or used during the study are available in a repository or online.

Reference

[1] S. Ghorbanzadeh and E. Lakzian, A numerical comparison between ejector performance with convergence and convergence-divergence primary nozzle, Modares Mechanical Engineering, 16(1), (2016), p. 324-332. https://doi.org/20.1001.1.10275940.1395.16.1.22.5

[2] M. Babaeyan and M. Hojaji, Experimental investigation of the penetration effects of opposite dual protuberances on thrust vector of a supersonic C-D nozzle, Modares Mechanical Engineering, 19(7), (2019), p. 1741-1750. https://doi.org/20.1001.1.10275940.1398.19.7.12.8

[3] A. Sharafi and D. Mokhtari, Experimental Study of Effect of Obstacle Presence and its Geometry on Thrust Vector and Outlet Jet in a Convergent-Divergent Micro Nozzle, Modares Mechanical Engineering, 20(5), (2020), p. 1211-1221. https://doi.org/20.1001.1.10275940.1399.20.5.14.3

[4] M.M. Fakhari, H.R. Bokaei and B. Shahriari, Numerical and Experimental Investigation of the Effect of Nozzle Divergent Section Geometry on Fluid Flow and Heat Transfer within the Nozzle, Modares Mechanical Engineering, 20(2), (2020), p. 467-473. https://doi.org/20.1001.1.10275940.1398.20.2.24.3

[5] N. Rahaei, I. Jafari Gavzan and R. Rafee, Investigation of Transient Heat Transfer inside Walls of Convergent-Divergent Nozzle, Journal of Solid and Fluid Mechanics, 10(3), (2020), p. 245-263. https://doi.org/10.22044/jsfm.2020.9212.3081

[6] S.A. Khan, O.M. Ibrahim and A. Aabid, CFD analysis of compressible flows in a convergent-divergent nozzle, Materials Today: Proceedings, 46(7), (2021), p. 2835-2842. https://doi.org/10.1016/j.matpr.2021.03.074

[7] A. Mahmoodi and R. Rafi, Effect of nozzle geometry on its performance in off-design mode in shock flow and boundary layer separation, Journal of Mechanical Engineering, 51(2), (2021), p. 205-213. https://doi.org/10.22034/jmeut.2021.10468

[8] S. Afkhami, N. Fouladi and M. Pasandideh Fard, Numerical Simulation of Flow Separation in a Thrust Optimized Parabolic Nozzle, Amirkabir Journal of Mechanical Engineering, 54(5), (2022), p. 985-1006. https://doi.org/10.22060/mej.2022.20465.7235

[9] A. Esmaeili, A. Pourtaghi, F Farhang and M. Dehnad, Investigation effect of the expansion ratio and propellant specifications on performance parameters of a nozzle and validation using experimental test, Fluid Mechanics & Aerodynamics, 10(2), (2022), p. 185-194. https://doi.org/20.1001.1.23223278.1400.10.2.10.7

[10] M. Hojaji, S. M. H. Razavi Dehkordi, S. A. Hosseini, M. Pourmohammadi and M. norouzi, Experimental investigation of the effects of secondary flow injection on the output flow of the convergent-

divergent nozzle at different beveled angles, Journal of Aeronautical Engineering, 24(1), (2022), p. 45-56. https://doi.org/10.22034/joae.2022.316243.1072

[11] M. Arznin and M Nimafar, Effects of radius of curvature and divergence angle on Mach number and static pressure in a convergent-divergent nozzle, 2th Conference on Electrical, Mechanical, Aerospace, Computer and Engineering Sciences, 2023.

[12] H.R. Farshi Fasih and M.H. Kamrava, Numerical investigation of the effect of nozzle throat wear on the performance of fluid flow inside a specific convergent-divergent nozzle, 31st Annual International Conference on Iranian Mechanical Engineering and 9th Iranian Power Plant Industry Conference, Tehran, 2023.

[13] A. Pourtaghi Marzrood, A. Esmaeili, A. Pourtaghi marzrood and M. Shameli, Investigating propellant flow in the converging-diverging nozzle with atmospheric outlet conditions by means of numerical simulation and validating the results with experimental tests, Space Science, Technology and Applications, 3(1), (2023), p. 87-96. https://doi.org/10.22034/jssta.2023.389896.1116

[14] S. Hamidi and M. J. Kermani, Numerical analysis of moist-air flow in converging-diverging nozzle with equilibrium and non-equilibrium thermodynamic models, Amirkabir Mechanical Engineering Journal, 55(9), (2023), p. 1113-1134. https://doi.org/10.22060/mej.2023.21836.7526

[15] S. A. Bagherzadeh, S. Emami Koopaei and S. A. Salehi, Optimal Design of Divergent Part of an Over-expanded Nozzle Profile using Artificial Intelligence, Journal of Applied and Computational Sciences in Mechanics, 35(1), (2023), p. 19-36. https://doi.org/10.22067/jacsm.2022.78011.1134

[16] M. Mohamad Hassan Zade, M. Hashem Abadi and J. Pirkandi, Numerical simulation of thrust vector control in convergent-divergent nozzles from the perspective of exergy and entropy, Journal of Mechanical Engineering, 55(3), (2025), p. 21-30. https://doi.org/10.22034/jmeut.2025.62789.3446

[17] S. A. I. Bellary, S. A. Dabir, S. A. Khan, T. Tamhane, J. H. Shaikh, & A. Khan, Computational Analysis of Thrust Generated by Converging Diverging Nozzle at Different Diverging Angle, Journal of Advanced Research in Numerical Heat Transfer, 29(1), (2025), p. 102-128. https://doi.org/10.37934/arnht.29.1.102128

[18] S. Guangtao, X. Jinglei, L. Zheng, G. Jianhui and X. Weijian, Experimental study of influence of twin-jet interaction on over-under combined nozzle performance, Chinese Journal of Aeronautics, 38(12), (2025). https://doi.org/10.1016/j.cja.2025.103642

[19] O. Teixeira, J. Páscoa and C. Purpura, Numerical model validation and aerodynamic MHD performance assessment with novel designs of contoured nozzles for hypersonic plasma wind tunnel testing, Aerospace Science and Technology, 164, (2025). https://doi.org/10.1016/j.ast.2025.110439

[20] Y. Narimani, A. Joulaei, A. Shirvani, M. Nili-Ahmadabadi and M.Y. Ha, Shape optimization of annular transonic thrust nozzles via genetic algorithm and adjoint method, Results in Engineering, 22, (2024),102255. https://doi.org/10.1016/j.rineng.2024.102255